

Structural Properties and Electrical Characteristics of High- κ Lu₂O₃ and Lu₂TiO₅ Gate Dielectrics for InGaZnO Thin-Film Transistors

Tung-Ming Pan*, Ching-Hung Chen, Hong-Jun Wang, and I-Chin Huang

Department of Electronic Engineering, Chang Gung University, 259 Wen-Hwa 1st rd., Gueishan, Taoyuan, Taiwan 33302
Tel: +886-3-211-8800 ext. 3349, Fax:+886-3-211-8507, Email:tmpan@mail.cgu.edu.tw

Abstract

We compared the structural and electrical properties of high- κ Lu₂O₃ and Lu₂TiO₅ gate dielectrics for indium-gallium-zinc oxide (InGaZnO) thin-film transistor (TFT) applications. In comparison of the Lu₂O₃ dielectric, the InGaZnO TFT using the Lu₂TiO₅ gate dielectric exhibited a lower threshold voltage of 0.25 V, a higher I_{on}/I_{off} current ratio of 1.3×10^8 , a smaller subthreshold swing of 130 mV/decade, and a larger field-effect mobility of 24.4 cm²/V-s. These results are probably due to the incorporation of TiO_x into the Lu₂O₃ film to form a Lu₂TiO₅ structure featuring a smooth surface, a low moisture absorption, a high dielectric constant, and a low interface state density at the oxide/channel interface.

1. Introduction

Amorphous indium-gallium-zinc oxides (InGaZnOs) have attracted much attention as active channel layers in switching thin-film transistors (TFTs) for transparent electronic, active-matrix organic light-emitting diode (OLED) display and liquid-crystal display applications [1]. This is due to their high field-effect mobility (μ_{FE}), low leakage current, good uniformity, high transparency, and low processing temperature [2]. A high gate dielectric capacitance is necessary to enable the required drive currents and to achieve a low operating voltage. Lu₂O₃ film is a potential material for fabricating the gate dielectric in application of CMOS because of its highest lattice energy (-13,871 kJ/mol) and the largest band gap (5.5 eV) [3-4]. Exposure to air, however, results in hygroscopic rare-earth oxides to react with moisture to form hydroxides [5], causing lower values of κ . The incorporation of Ti or TiO_x films into rare-earth oxides increases their stability toward moisture [6].

2. Device Fabrication

Figure 1 represents the schematic cross-section view of the high- κ Lu₂O₃ and Lu₂TiO₅ InGaZnO TFT devices. Back-gated InGaZnO TFT devices were fabricated on thermally grown SiO₂ on Si substrate. A ~50-nm Lu₂O₃ film was deposited through reactive sputtering from a Lu target, while a ~50-nm Lu₂TiO₅ film was deposited by means of co-sputtering from both Lu and Ti targets. A 20-nm InGaZnO active layer was deposited by reactive sputtering at room temperature, using a target of In₂O₃:Ga₂O₃:ZnO= 1:1:1 mol %. Finally, the Al film source/drain electrodes were formed by a thermal evaporation system and then patterned in channel width/length (W/L) dimension of 50 μ m/5 μ m by lift-off process.

3. Results and Discussion

Fig. 2 shows the crystalline structures of the Lu₂O₃ and Lu₂TiO₅ films. One strong Lu₂O₃ (400) peak was observed in the Lu₂O₃ film, while one relatively weak Lu₂TiO₅ (102) peak for the Lu₂TiO₅ sample. Fig. 3 depicts that the surface roughness of Lu₂O₃ film is about three times larger than that of Lu₂TiO₅ film. Fig. 4 shows the Lu 4f XPS spectra of the Lu₂O₃ and Lu₂TiO₅ films. The Lu 4f peak of the reference Lu₂O₃ located at 8 eV [7]. The Lu 4f peak of the Lu₂TiO₅ film shifted higher binding energy by 0.4 eV as compared with the Lu₂O₃ reference position. Fig. 5 displays the O 1s spectra of the Lu₂O₃ and Lu₂TiO₅ films with appropriate curve-fitting of peaks. In the three sets of spectra, the O 1s peaks at 532.1, 530.1, and 529.6 eV correspond to the Lu-OH [8], Lu-O-Ti, and Lu-O [7] bonds, respectively. Fig. 6 shows the C-V curves of the Al/Lu₂O₃/TaN and Al/Lu₂TiO₅/TaN MIM capacitors. The capacitance density of Al/Lu₂TiO₅/TaN device exhibited larger compared with Al/Lu₂O₃/TaN one. The κ value of the Lu₂O₃ and Lu₂TiO₅ dielectric films is evaluated to be 12.5 and 16.1, respectively. Fig. 7 depicts that the Al/Lu₂TiO₅/TaN device exhibited a slightly higher leakage current than the Al/Lu₂O₃/TaN one. This result is attributed to the low electron barrier height of the Al/Lu₂TiO₅ and Lu₂TiO₅/TaN contacts.

Fig. 7 demonstrates the transfer characteristics and field-effect mobilities as a function of V_{GS} for the proposed InGaZnO TFT devices featuring high- κ Lu₂O₃ and Lu₂TiO₅ gate dielectrics. The InGaZnO TFT using the Lu₂TiO₅ gate dielectric exhibits a lower V_{TH} (from 0.43 to 0.25 V), higher I_{on}/I_{off} current ratio (from 3.5×10^6 to 1.3×10^8), steeper SS (from 276 to 130 mV/decade), and higher μ_{FE} (from 14.5 to 24.4 cm²/V-s) as compared with the Lu₂O₃ one. Fig. 7 shows the output characteristics of the high- κ Lu₂O₃ and Lu₂TiO₅ InGaZnO TFT devices. The InGaZnO TFT device using a Lu₂TiO₅ gate dielectric exhibited a larger driving current than that of Lu₂O₃ dielectric, suggesting the higher mobility and smaller threshold voltage.

3. Conclusions

We compared the structural and electrical properties of Lu₂O₃ and Lu₂TiO₅ dielectric films for InGaZnO TFT applications. We used XRD, AFM, and XPS analyses to confirm the presence of Lu₂O₃ and Lu₂TiO₅ structures in these TFT devices. The InGaZnO TFT device incorporating a Lu₂TiO₅ gate dielectric exhibited better electrical characteristics, such as a low threshold voltage of 0.27 V, a large field-effect mobility of 24.4 cm²/V-s, a high I_{on}/I_{off} ratio of 1.3×10^8 , and a small SS of 130 mV/decade, in comparison

with that of Lu_2O_3 dielectric. We attribute this behavior to the Lu_2TiO_5 film forming a smooth surface, possessing a low moisture absorption, featuring a high κ value, and reducing an interface state density at the oxide/channel interface.

References

[1] K. Nomura, et al., *Nature*, vol. 432, p. 488, 2004.
 [2] T. Kamiya et al., *Sci. Technol. Adv. Mater.*, vol. 11, p. 044305, 2010.

[3] H. Iwai et al., *Tech. Dig. - Int. Electron Devices Meet.* 2003, p. 625.
 [4] P. Darmawan et al., *J. Vac. Sci. Technol. B*, vol. 25, p. 1203, 2007.
 [5] Y. Zhao et al., *Appl. Phys. Lett.*, vol. 88, p. 072904, 2006.
 [6] R. B. van Dover, *Appl. Phys. Lett.*, vol. 74, p. 3041, 1999.
 [7] Y. A. Teterin and A. Yu. Teterin, *Russ. Chem. Rev.*, vol. 71, p. 347, 2002.
 [8] G. Scarel et al., *Appl. Phys. Lett.*, vol. 85, p. 630, 2004.

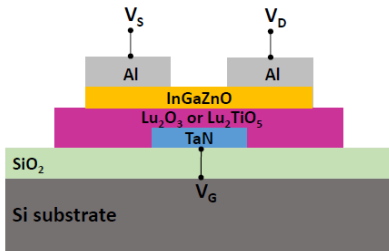


Fig. 1 Schematic view of the high- κ Lu_2O_3 and Lu_2TiO_5 InGaZnO TFT devices.

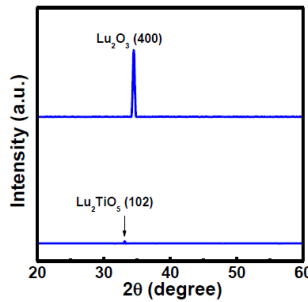


Fig. 2 XRD patterns of Lu_2O_3 and Lu_2TiO_5 dielectric films.

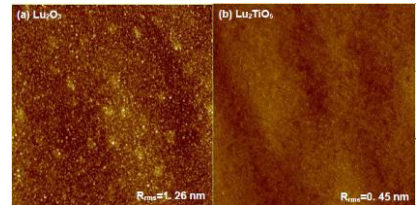


Fig. 3 AFM surface images of (a) Lu_2O_3 and (b) Lu_2TiO_5 films.

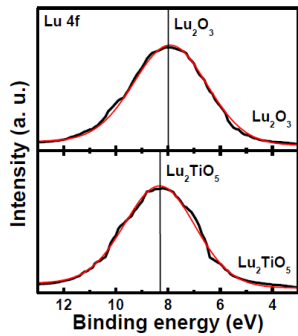


Fig. 4 XPS spectra of Lu 4f for Lu_2O_3 and Lu_2TiO_5 dielectric films.

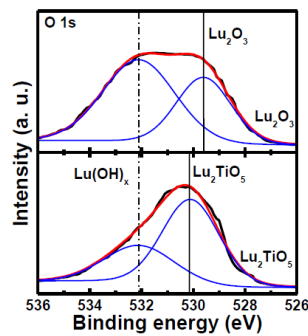


Fig. 5 XPS spectra of O 1s for Lu_2O_3 and Lu_2TiO_5 dielectric films.

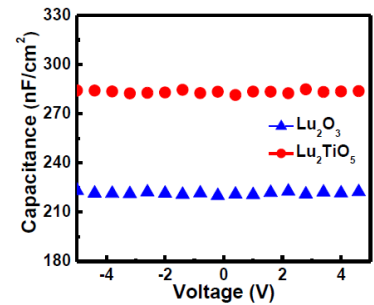


Fig. 6 Capacitance-voltage of Al/ Lu_2O_3 /Ta N and Al/ Lu_2TiO_5 /Ta N capacitors.

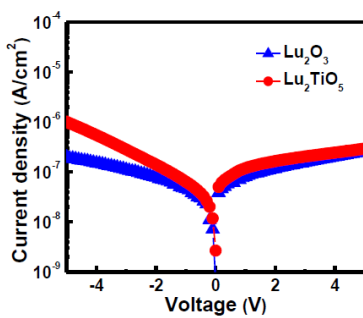


Fig. 7 Current-voltage characteristics of Al/ Lu_2O_3 /Ta N and Al/ Lu_2TiO_5 /Ta N capacitors.

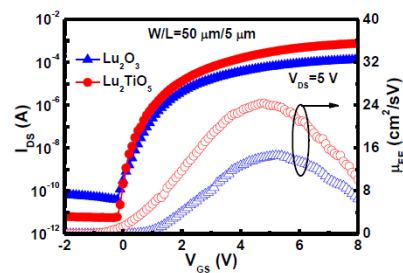


Fig. 8 Transfer ($I_{\text{DS}}-V_{\text{GS}}$) characteristics of high- κ Lu_2O_3 and Lu_2TiO_5 InGaZnO TFT devices.

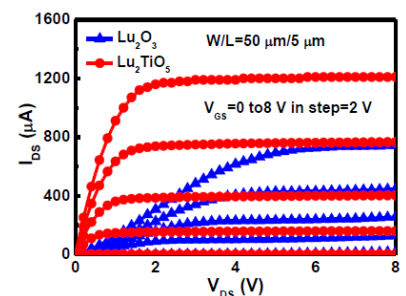


Fig. 9 Output ($I_{\text{DS}}-V_{\text{DS}}$) characteristics of high- κ Lu_2O_3 and Lu_2TiO_5 InGaZnO TFT devices.